Requirement for Scleraxis in the recruitment of mesenchymal progenitors during embryonic tendon elongation

Alice H. Huang[1,2], Spencer S. Watson[1], Lingyan Wang[3], Brendon Baker[4], Haruhiko Akiyama[5], John V. Brigande[3], Ronen Schweitzer[1]

[1] Research Division, Shriners Hospital for Children, Portland, OR 97239
[2] Department of Orthopaedics, Icahn School of Medicine at Mount Sinai, New York, NY 10029
[3] Oregon Hearing Research Center, Oregon Health & Science University, Portland, OR 97239
[4] Department of Biomedical Engineering, University of Michigan, Ann Arbor, MI 48109
[5] Department of Orthopaedics, Gifu University, Gifu City JAPAN

Corresponding Authors:

Alice Huang, PhD
Associate Professor
Dept of Orthopaedics, Icahn School of Medicine at Mount Sinai
1 Gustave Levy Pl, Box 1188
NY, NY 10029

Phone: (212) 241-1158
Email: alice.huang@mssm.edu

Ronen Schweitzer, PhD
Associate Professor
Research Division, Shriners Hospital for Children
3101 SW Sam Jackson Park Road
Portland, OR 97239

Phone: (503) 221-3437
Email: schweitz@ohsu.edu

Date: 8/28/2019
Keywords: tendon development, musculoskeletal, scleraxis, mouse

Abstract

The transcription factor *Scleraxis* (*Scx*) is required for tendon development; however, the function of *Scx* is not fully understood. Although *Scx* is expressed by all tendon progenitors and cells, only long tendons are disrupted in the $Scx^{-/-}$ mutant while short tendons appear normal and the ability of muscle to attach to skeleton is not affected. We recently demonstrated that long tendons are formed in two stages: first by muscle anchoring to skeleton via a short tendon anlage, followed by rapid elongation of the tendon in parallel with skeletal growth. Through lineage tracing, we extend these observations to all long tendons and show that tendon elongation is fueled by recruitment of new mesenchymal progenitors. Conditional loss of *Scx* in mesenchymal progenitors did not affect the first stage of anchoring; however, new cells were not recruited during elongation and long tendons failed to form. Interestingly, for tenocyte recruitment, *Scx* expression was required only in the recruited cells and not in the recruiting tendon. The phenotype of *Scx* mutants can thus be understood as a failure of tendon cell recruitment during tendon elongation.

Introduction

Development of the limb musculoskeletal system requires the coordinated differentiation and growth of the skeleton, muscles, and tendons, however, the patterning cues and mechanisms that allow for integrated development are largely unknown. While it is well established that the primary skeletal structures (i.e., the long bones) and muscles can form independently of one another, a growing body of evidence suggests that the formation of tendons requires signals from the adjacent skeletal and muscle tissues (Arvind and Huang, 2017; Blitz et al., 2009; Chen and Galloway, 2014; Edom-Vovard and Duprez, 2004; Huang, 2017; Kardon, 1998). Tendon function in integrating muscle and skeleton into a unified system suggests that the regulation of tendon growth may be a key mechanism by which the musculoskeletal system maintains coordinated growth to establish proportions optimal for mechanical tension and force transfer. Despite the functional importance of tendons, however, there is still very little known about the cell and molecular events that regulate their growth and development.

In the mouse limb, the distal skeletal segments are controlled by long tendons that extend from muscles in the arm (zeugopod) and insert into skeletal sites within the wrist or paw (autopod) (Watson et al., 2009). Autopod and zeugopod tendons are formed as separate modular units that are independently regulated, such that tendons in one segment can develop in the absence of tendons in the other segment (Huang et al., 2015; Kardon, 1998). While autopod tendon induction depends on cartilage, the zeugopod tendon components are first induced at E12.5 as short-range progenitors anchoring muscle to the skeleton, followed by tendon differentiation and elongation in parallel with skeletal growth. In the absence of muscle, zeugopod tendon induction is initiated, but subsequent differentiation and growth fails at E13.5 and the tendon anlagen are lost (Huang et al., 2015). This biphasic mode of long tendon development (anchoring and elongation) provides a useful framework on the tissue level, but the cellular dynamics and molecular regulators of this process have not been established.

One intriguing marker for tendon is the transcription factor *Scleraxis* (*Scx*), which is expressed by all tendon progenitors and cells, yet its functional role in tendon development remains poorly understood (Murchison et al., 2007; Schweitzer et al., 2001; Yoshimoto et al., 2017). The *Scx*$^{-/-}$ mutant displays a strong tendon phenotype; however, not all tendons are equally affected (Murchison et al., 2007). The long-range tendons of the trunk and limbs are either missing or severely deficient, but short-range anchoring tendons appear normal. Importantly, the ability of tendon to connect muscle to skeleton is not impaired in the absence of *Scx*, since the *Scx*$^{-/-}$ mutant is viable past birth, despite limited mobility due to disruption of the long tendons. This suggests that *Scx* may be functionally important for tendon growth and elongation.

One paradigm underlying tissue and organ development follows a basic assumption that progenitor cells are specified at an early stage and that these cells then differentiate and proliferate to form the final tissue/organ (Gilbert, 2010). There is emerging evidence, however, suggesting that this simple paradigm is not applicable for all tissues/organs. In the joint, it was shown that joint progenitor cells may be continuously induced and allocated (Shwartz et al., 2016). In this study, we show that tendon elongation in the mouse limb and tail is fueled by recruitment of new mesenchymal progenitors. We further find that *Scx* is not required for tendon anchoring, but *Scx* expression in mesenchymal progenitors is required for their recruitment during tendon elongation, underlying the disruption of long tendons in the *Scx* mutant.

Results

Long tail tendons develop via establishment of a short-range tendon anlage followed by tendon elongation.

Integration of the musculoskeletal tissues is first established at E12.5 when short-range anchoring tendons attach muscles to the skeleton. Subsequent elongation of the short-range tendon anlage

into the zeugopod allows for coordinated development of all musculoskeletal elements during growth (Huang et al., 2015). Although this model was initially conceptualized based on observations in limb tendon development, the limb as a model system poses additional challenges for mechanistic studies due to the complex patterning of several tendons (which are initially formed as fused units that subsequently separate) as well as the modular nature of the autopod and zeugopod segments during tendon development (Huang et al., 2015; Watson et al., 2009). To bypass these complexities, we turned to the tail tendons as a simplified model system to identify the cell and molecular mechanisms underlying anchoring and elongation. Tail tendons are also advantageous since they are the longest tendons in the body and undergo the most dramatic growth during development.

The fully formed mouse tail consists of long tendons that extend from muscles that reside in the base of the tail to each vertebral bone within the tail (**Fig. 1A**) (Shinohara, 1999). Movement of each skeletal element is governed by dorsal and ventral tendons organized in quadrants (**Fig. 1A**, **B**). Since all tendons extend from muscles at the base of the tail, the tendons that insert closest to the tip of the tail are much longer than those that insert closer to the base. To determine whether tail tendon development is governed by similar principles of anchoring and elongation, we examined the early stages of tail development. Whole mount confocal imaging of E13.5 *ScxGFP* embryos showed repeating short-range *ScxGFP+* tendon segments along the tail, attached to their respective vertebral structures (**Fig. 1C**). The shortest tendon segments were found closest to the tip of the tail (white arrow). Whole mount immunostaining for myosin heavy chain for muscle showed that each of these short-range tendon segments is directly attached to muscle (**Fig. 1C', C"**). Between E13.0 and E15.5, there is dramatic elongation of these short-range tendon segments to form the long-range tendons of the tail, concurrent with skeletal growth (**Fig. 1D**). These results show that long tail tendons also undergo a developmental process of tendon anchoring followed by tendon elongation, similar to the long tendons of the limb.

Sox9 lineage tracing shows tail tendon elongation is driven by recruitment of new tendon progenitors.

Having established that long tail tendons undergo elongation, we next examined the cellular basis for tendon elongation and asked whether the cells driving tendon elongation are completely derived from the early population of anlage progenitors or whether there is subsequent recruitment of new cells. To address this question, we used $Sox9^{Cre}$ to distinguish early tendon progenitors since it was previously demonstrated that the cells forming the early skeletal insertion site are derived from bipotent *Scx+/Sox9+* progenitors, established at E12.5 (Blitz et al., 2013; Sugimoto et al., 2013). The transient expression of *Sox9* in early tendon progenitors and the consistent localization of *Sox9*-lineage ($Sox9^{lin}$) tendon cells to regions near the skeletal insertion suggested that in tendon *Sox9* may be a distinctive marker for the anchoring anlagen progenitors. We therefore examined the tails of $Sox9^{Cre}$ embryos combined with the *Rosa26-TdTomato* (*RosaT*) Cre reporter at E12.5. Imaging by whole mount confocal microscopy and in transverse sections showed that the *ScxGFP*+ tail tendon anlagen are completely derived from *RosaT*+, $Sox9^{lin}$ cells, demonstrating that *Sox9* is indeed a useful marker for the anchoring tendon in the tail (**Fig. 2A, B-B", C-C"**).

Since the early tail tendon anlagen is composed of $Sox9^{lin}$ progenitors, we used the inducible $Sox9^{CreERT2}$ mutant to label these cells at E12.5 via tamoxifen injection and determine whether new tendon progenitors are recruited during tendon elongation. To evaluate the distribution of labeled cells along the tendon, we focused our analyses to two distinct regions in the tail in order to (1) follow individual tendons as they insert into the skeleton as well as (2) capture tendons well away from their skeletal insertions. Since tail tendons are extremely long and numerous (**Fig. 1**), we determined that the best region to follow individual tendons as they insert was close to the tail tip (since most of the other tendons would have already inserted proximally). A series of consecutive transverse sections taken across the length of the tail tip at E16.5 showed that tendon cells further from the insertion (tendon #5, L1) are devoid of $Sox9^{lin}$ cells while tendon cells near/at the insertion

(tendon #1, L1 and L2; tendon #2, L3 and L4) are strongly composed of *Sox9*^{lin} cells (**Fig. 2D, E**). To confirm that tendon cells away from the skeletal insertions are non-*Sox9*^{lin}, we also collected sections closer to the tail base where the tendons attach to muscle. Analysis of these sections revealed that the bulk of the tendon midsubstance length is almost completely derived from non-*Sox9*^{lin} cells (*ScxGFP*+, *RosaT*-), indicating that tendon elongation is likely fueled by recruitment of new progenitors and not by expansion of the original anchoring population (**Fig. 2F, G**).

Since previous studies showed dramatic variability in the contribution of *Sox9*^{lin} cells in tendons (Soeda et al., 2010), we also examined *Sox9*^{Cre}-labeled tail tendons at E16.5 in transverse sections. To our surprise, *Sox9*^{Cre} lineage tracing showed that the full length of dorsal tail tendons (from skeletal insertion to muscle origin) is almost entirely composed of *Sox9*^{lin} cells (**Fig. S1**). Notably, ventral tail tendons were composed of largely non-*Sox9*^{lin} cells, which suggested that *Sox9* itself is likely not playing a functional role in tendon development (**Fig. S1**). This is also supported by other studies showing that deletion of *Sox9* by *Scx*^{Cre} does not result in loss of tendon (Blitz et al., 2013). Collectively, the analyses of *Sox9*^{CreERT2} and *Sox9*^{Cre} tail tendons indicate that the anchoring tendon is initially composed of *Sox9*^{lin} cells, while new tendon progenitors are subsequently recruited during tendon elongation. In addition, these progenitors may be either *Sox9*^{lin} or non-*Sox9*^{lin}.

<u>Conditional deletion of *Scx* shows that *Scx* is required in mesenchymal cells to enable their recruitment during tail tendon elongation.</u>

Since both the anchoring tendon progenitors and the recruited mesenchymal cells in dorsal tendons are derived from *Sox9*^{lin} progenitors, we next tested *Scx* function using *Sox9*^{Cre} to target both cell populations in dorsal tendons. In *Scx*$^{-/-}$ mutants, tail tendons are severely disrupted. If *Scx* is required in anchoring progenitors, we expected *Scx*^{Sox9Cre} mutants to phenocopy *Scx*$^{-/-}$ mutants in that new cells will not be recruited resulting in a failure of tendon elongation. Conversely, if *Scx* is required only in the recruited mesenchymal cells, then mutant cells will be excluded from the

elongating tendon. When we examined transverse sections of tails from *Scx*^{Sox9Cre} *; RosaT* embryos at E18.5, we found that dorsal tail tendons were still present, however the mutant tendons were much smaller than wild type tendons (**Fig. 3A-D**). Analysis of *RosaT* expression showed that mutant dorsal tendons at the midsubstance were almost completely composed of non-*Sox9*^{lin} cells (**Fig. 3C, D**). Remarkably, these data showed that out of a large population of mutant cells (*RosaT*+), only wild type cells were capable of recruitment, suggesting that *Scx* is required in mesenchymal cells for their recruitment into tendon. Reduced dorsal tendon size in the mutant was likely a result of the restricted availability of wild type cells in the surrounding milieu, since in WT embryos these tendons are fully composed of *Sox9*^{lin} cells. Moreover, since the anchoring tendon is targeted by Sox9^{Cre} this result also indicates that *Scx* function is required exclusively in the recruited mesenchymal cells and not in the recruiting tendon, since loss of *Scx* in the anchoring tendons in the dorsal tail tendons of these mutants did not preclude cell recruitment. Interestingly, the size of ventral tendons (which normally recruit a mix of *Sox9*^{lin} and non-*Sox9*^{lin} cells) appeared relatively normal in *Scx*^{Sox9Cre} mutants, which may be due to the larger availability of wild type cells in the vicinity of these tendons (**Fig. S1**).

Conditional deletion and embryonic cell injections show that *Scx* is required for tendon cell recruitment in the limb.

Our experiments in the mouse tail showed that tendon elongation is fueled by recruitment of new cells and that *Scx* is required for their recruitment. To determine whether this is a general mechanism for long tendon growth, we evaluated the complex tendons within the limb by whole mount confocal imaging. Initial analyses of *Sox9*^{Cre}*; RosaT; ScxGFP* limbs showed broad Cre activity in a variety of tissues, including skin and nerves; as a result, *RosaT* expression was overwhelming in maximum intensity projections and did not reflect true *Sox9*^{lin} cell contribution to tendon (**Fig. S2**). We therefore developed a non-biased approach using customized algorithm in Matlab software to eliminate the *RosaT* signal in *ScxGFP*-negative cells, thereby restricting *RosaT* signal to tendon and

related connective tissues (**Fig. 4A, B**). Analysis of *Sox9^{lin}* cells in limb tendons of *Sox9^{Cre}; RosaT* embryos at E12.5 revealed that the short range tendon anlage that mediate connections between skeleton and muscle are highly composed of *Sox9^{lin}* cells, similar to our findings for the E12.5 tail. Interestingly, the short range tendons that integrate the muscles in the zeugopod with their respective autopod tendons are also highly composed of *Sox9^{lin}* cells (**Fig. 4A, Fig. S3**). The *Sox9^{lin}* population in tendons was largely restricted to the wrist where the muscles attached, and the autopod components of these tendons were composed of mixed or non- *Sox9^{lin}* cells. When we evaluated *Sox9^{Cre}; RosaT* embryos at a later stage (E16.5), we found mixed composition of *Sox9^{lin}* and non-*Sox9^{lin}* cells in most tendons within the zeugopod, although the tendon regions near the wrist and elbow remained strongly *RosaT*+ for most tendons (**Fig. 4B, 4C**). Tamoxifen labeling of *Sox9^{lin}* cells at E12.5 showed that most of the tendon at E16.5 was derived from recruited cells, similar to the distribution in the tail tendons (**Fig. 4D**). Deletion of *Scx* in *Sox9^{lin}* cells using *Sox9^{Cre}* resulted in a dramatic exclusion of mutant cells from the zeugopod tendons, similar to the phenotype observed in the tail (**Fig.5**). Limb tendon diameters were noticeably smaller, although not to the same extent as the mutant dorsal tail tendons.

Although the data was highly suggestive, the mixed composition of *Sox9^{lin}* and non-*Sox9^{lin}* cells in limb tendons prompted us to test the role of cell recruitment and *Scx* function via an additional experimental approach by injecting lableled mesenchymal cells into developing limbs *in utero* and testing the recruitment of such cells into developing tendons. To label limb mesenchyme we used the *Prx1^{Cre}* driver that targets all cells in the early limb bud mesenchyme. We isolated *RosaT*+ mesenchymal cells from *Prx1^{Cre}; RosaT; ScxGFP* limb buds at E12.5, and directly injected these cells into the limb buds of stage matched *ScxGFP* embryos via transuterine microinjection (**Figure 6A**). Since only donor cells are labeled, the presence of *RosaT*+ cells incorporated within a tendon would indicate cell recruitment. Location alone was not sufficient for a *RosaT*+ cell to be considered recruited however, unless the labeled cell also adopted a tenogenic fate by expressing *ScxGFP*.

Systematic analysis of consecutive transverse sections taken from digit to elbow showed numerous examples of non-recruited donor cells embedded within the mesenchyme that were not associated with any tendon and did not express *ScxGFP* (white arrows, **Fig. 6B-B', C-C'**). Occasionally however, donor cells expressing *ScxGFP* were found within tendon, matching our criteria for recruitment (yellow arrows, **Figure 6B, B'**). Out of 26 WT injected embryos, 7 embryos had at least one positive recruitment event. Positive recruitment involved only one or two cells and was not limited to any particular tendon or region within a tendon.

Having demonstrated cell recruitment into tendons using transuterine cell injection, we next wanted to test *Scx* role in this experimental paradigm. Injecting $Scx^{-/-}$ mutant cells into WT limbs would closely parallel the genetic experiments described above. However, since we found that injection of WT cells into WT limbs resulted in modest recruitment efficiency (WT-WT, ~27%), a very large number of injections would be required to determine a definitive failure of the recruitment of $Scx^{-/-}$ cells. We therefore opted to perform the complementary experiment by injecting labeled WT cells into $Scx^{-/-}$ mutant limbs (WT-Mutant) (**Fig. 6D**). When WT cells were injected into mutant limbs we found that 100% of limbs (4/4) showed positive recruitment events. Moreover, while positive recruitment in the WT-WT experiments were typically 1-2 cells within a tendon, positive recruitment events in WT-Mutant consisted of massive incorporation of WT cells (**Fig. 6E'-E", F-F', G-G'**). Whole mount imaging showed extensive *RosaT*+ signal within tendon, which was confirmed via transverse sections showing large numbers of recruited cells for several consecutive sections, highlighting preferential recruitment of injected WT cells in an environment where most mesenchymal cells are $Scx^{-/-}$ and therefore cannot be recruited to the tendon. Collectively, these results indicate that cell recruitment is a driving force in tendon elongation and that *Scx* function is required in the mesenchymal cells that are recruited. The ability of $Scx^{-/-}$ tendons to recruit WT cells further shows that for cell recruitment, *Scx* activity is required exclusively in the recruited cells and there is no role for *Scx* activity in the recruiting tendon.

Discussion

In this study, we showed that the long tendons in the body are typically formed by anchoring and elongation and further identified a fundamental mechanism underlying elongation. We show that there is addition of mesenchymal cells recruited after induction of the anchoring tendon, which fuels the dramatic extension of long tendons during growth. In addition, *Scx* expression in mesenchymal cells is required for their recruitment, thus establishing a new and critical function for this essential tendon transcription factor (**Fig. 7**).

Scx was the first transcription factor identified for tendons, and to date remains the earliest known marker for distinguishing tendon and connective tissue progenitors during embryonic development (Chen and Galloway, 2014; Schweitzer et al., 2001). The early and distinctive expression of *Scx* initially suggested that *Scx* may be a master regulator of the tendon cell fate, however, analyses of the $Scx^{-/-}$ mutant subsequently revealed that tendons can still develop in the absence of *Scx*, although many of the tendons are grossly impaired (Murchison et al., 2007; Schweitzer et al., 2001). One confounding aspect of the $Scx^{-/-}$ mutant was the divergent phenotypes of two types of tendons, which can be generally classified as short-range and long-range tendons. While short-range tendons (such as the intrinsic lumbrical tendons of the autopod or the flattened tendon sheets connecting the intercostal muscles to the ribs) are completely unaffected in the $Scx^{-/-}$ mutant, long-range tendons (such as the long tendons of the limbs and tail) are severely reduced or missing. In the context of long tendon formation, we now demonstrate that the $Scx^{-/-}$ phenotype is a failure of tendon elongation, and more specifically, a failure of tendon cell recruitment during elongation. This is consistent with our previous results, which showed normal tendon induction at E12.5 in the $Scx^{-/-}$ mutant (during the stage of tendon anchoring), with the manifestation of the tendon phenotype at E13.5 (during the stage of tendon cell recruitment and elongation) (Murchison et al., 2007). In the current study, we also found that deletion of *Scx* in the early population of $Sox9^{lin}$ anchoring tendon

progenitors at E12.5 did not negate the ability of these cells to subsequently recruit wild type cells, further supporting the specific activity of *Scx* in the newly-recruited mesenchymal cells.

While we have identified this new and exciting function for *Scx*, it also plays other roles in tendon biology. For example, it was shown that *Scx* drives expression of *Col1a1*, and collagen matrix content is greatly reduced in $Scx^{-/-}$ tendons, indicating that *Scx* may also have a later role in tendon matrix synthesis (Lejard et al., 2007; Murchison et al., 2007). The loss of the flexor digitorum profundus tendons in the metacarpal regions of the autopod also suggests a failure of progenitor cell condensation, independent of tendon elongation. And finally, it was previously shown that *Scx* drives *BMP4* expression in bone eminence progenitor cells, which is required for cartilage differentiation to form the secondary skeletal structures, such as bone ridges and tuberosities (Blitz et al., 2013; Blitz et al., 2009).

Although we used for this study expression of *Sox9* as a fortuitous marker of early tendon progenitor cells, we found no evidence for a functional role for *Sox9* in either tendon cell anchoring or recruitment during elongation. This is consistent with previous reports, which showed that long tendons are not noticeably disrupted in $Sox9^{ScxCre}$ mutants, although the skeletal enthesis and tuberosities were lost. In both our tail and limb models, $Sox9^{lin}$ and non-$Sox9^{lin}$ cells can be recruited into tendons. However, while the composition of $Sox9^{lin}$ cells varied dramatically between tendons, the relative composition of $Sox9^{lin}$ cells was remarkably constant for each tendon. For example, the dorsal tendons of the tail are always highly composed of $Sox9^{lin}$ cells, while the ventral tendons are of mixed composition, suggesting that cell recruitment is likely driven by proximity of mesenchymal cells to the growing tendon. In cases where most surrounding cells are from a $Sox9^{lin}$, the tendon would be heavily composed of such cells. Consistent with this hypothesis, in the $Scx^{Sox9Cre}$ mouse where *Scx* mutant cells are no longer recruited, tendon size is reduced only in tendons that normally incorporate a large number of $Sox9^{lin}$ cells. Consequently, the tendon phenotype of $Scx^{Sox9Cre}$ is

significantly milder than that of *Scx*$^{-/-}$ tendons in which several long tendons are lost (including all of the long tendons of the tail), likely due to the ability of *Scx*^{Sox9Cre} tendons to still recruit wild type cells and maintain structural integrity.

The long tendons of the limb and body are a common anatomic feature in mammalian species, but are not universal across tetrapod clads. In more primitive vertebrates such as amphibians, the zeugopod and tail are highly muscular and short tendons mediate the attachment of these muscles to the skeleton (Diogo et al., 2009) (Ashley-Ross, 1992; Diogo et al., 2009; Walthall and Ashley-Ross, 2006). While long tendons are observed in the amphibian autopod, the developmental program governing the autopod tendons is distinct from that of the long zeugopod tendons, and elongation of autopod tendons may involve divergent mechanisms (Huang et al., 2015). While cell recruitment appears to be a fundamental mechanism driving elongation, it is not clear whether recruitment is part of the original mechanism underlying all tendon formation or whether it is a later evolutionary addition specific to the new developmental program regulating long tendon elongation. From a functional perspective, the shift from short to long tendons may be advantageous. It has been shown that increasing the length of tendons relative to the length of muscle fascicles increases the energy storage capacity of tendons, enhancing muscle function while reducing the metabolic cost of muscle contraction (Alexander, 2002). Interestingly, cell recruitment does not occur as a substitute for tenocyte proliferation (which is sustained throughout the stages of tendon elongation), but is an additional mechanism for generating new cells. This indicates that proliferation alone may be insufficient for the tendon to keep pace with the growth of the underlying skeletal structures. The dramatic extension of the tendons during evolution may have necessitated a new, additional cellular mechanism for growth, to enable the remarkable increase (and variation) in limb length that occurred through mammalian evolution.

Methods

Mice

Existing mouse lines used in these studies were previously described: *ScxGFP* tendon reporter (Pryce et al., 2007), *Sox9^{Cre}* (Akiyama et al., 2005), *Sox9^{CreERT2}* (Soeda et al., 2010), *Scx$^{-/-}$* (Murchison et al., 2007), *Scx$^{f/f}$* (Murchison et al., 2007), *Prx1^{Cre}* (Logan et al., 2002), *Ai14 Rosa26-TdTomato* reporter (*RosaT*) (Madisen et al., 2010). All mice were crossed with *ScxGFP* to enable visualization of tendon cells.

Limb bud cell isolation and transuterine microinjection into E12.5 limbs

Stage-matched timed matings were set for donor embryos (*Prx1^{Cre}; RosaT; ScxGFP*) and host embryos (*ScxGFP* or *Scx$^{-/-}$; ScxGFP*). On the day of injection, *RosaT+; ScxGFP+* forelimb and hindlimb buds were isolated from E12.5 donor embryos and rinsed in sterile PBS. Limb bud cells were isolated by incubation in digestion solution (0.1% collagenase, 0.1% trypsin in PBS) at 37°C for 10 minutes. Cells were then resuspended in DMEM at a concentration of $1.5x10^6$ cells/mL and kept on ice until injection. For injections, the uterine horns of pregnant dams were externalized by ventral laparotomy and transilluminated to visualize the host E12.5 embryo (Gubbels et al., 2008; Huang et al., 2013; Wang et al., 2012). 10 nL of cell solution was microinjected through the uterus into the presumptive wrist region of the nascent limb. Host embryos with injected limbs were harvested at E14.5 and whole mount limbs were visually scanned for the presence of *RosaT*+ signal indicative of successful injection. Limbs showing any positive expression were then processed for histology and cryosectioned from digit tips to elbow. Every section was collected and inspected to identify recruited cells into tendon.

Histology

Standard protocols for whole mount and section immunostaining were performed as previously described (Murchison et al., 2007). Patterning of limb and tail tendons and muscles was acquired in serial transverse sections (Watson et al., 2009). A monoclonal antibody for My32 (Sigma), was used to detect muscle-specific type II myosin heavy chain (MHC).

Whole Mount Confocal Microscopy and Image Processing

Mouse forelimbs or tails from E12.5-E15.5 were fixed in 4% paraformaldehyde overnight at 4°C. Following fixation, whole mount immunostaining for MHC was carried out for E12.5 and E13.5 limbs and tails as previously described (DeLaurier et al., 2006). Tissues were then incubated in Sca/e2 solution at 4°C until cleared (Hama et al., 2011). The Zeiss LSM780 laser scanning confocal microscope was used to acquire 10x tiled z-stack images. Image processing was carried out using Zeiss Zen software to stitch tiles and obtain maximum intensity projection images. Transverse sections were imaged using the Zeiss AxioImager with Apotome for optical sectioning. Since *Sox9*^{Cre} labeling is broad in the limb, whole mount confocal *Sox9*^{Cre}*; RosaT; ScxGFP* images were processed using custom MATLAB software to eliminate non-*ScxGFP* contributions to better enable visualization of *Sox9*^{lin} cells in tendon.

Acknowledgements

This work was supported by NIH/NIAMS (R01AR055640, R01AR055973) and Shriners Hospital (85410-POR-14) grants to R.S.; funding from the Arthritis Foundation to A.H.H.; and by funding from NIH R01DC008595 to J.B.

Author Contributions

AHH, SW, and LW contributed to experiments and data collection. BB created custom image processing software in MATLAB for whole mount confocal images. HA generated the *Sox9*^{Cre} and *Sox9*^{CreERT2} mouse lines. AHH, JB, and RS contributed to conception, data analysis and interpretation. AHH and RS prepared the manuscript prior to submission.

References

Akiyama, H., Kim, J. E., Nakashima, K., Balmes, G., Iwai, N., Deng, J. M., Zhang, Z., Martin, J. F., Behringer, R. R., Nakamura, T., et al. (2005). Osteo-chondroprogenitor cells are derived from Sox9 expressing precursors. *Proc Natl Acad Sci U S A* **102**, 14665-14670.

Alexander, R. M. (2002). Tendon elasticity and muscle function. *Comp Biochem Physiol A Mol Integr Physiol* **133**, 1001-1011.

Arvind, V. and Huang, A. H. (2017). Mechanobiology of limb musculoskeletal development. *Ann N Y Acad Sci* **1409**, 18-32.

Ashley-Ross, M. A. (1992). The Comparative Myology of the Thigh and Crus in the Salamanders Ambystoma-Tigrinum and Dicamptodon-Tenebrosus. *Journal of Morphology* **211**, 147-163.

Blitz, E., Sharir, A., Akiyama, H. and Zelzer, E. (2013). Tendon-bone attachment unit is formed modularly by a distinct pool of Scx- and Sox9-positive progenitors. *Development* **140**, 2680-2690.

Blitz, E., Viukov, S., Sharir, A., Shwartz, Y., Galloway, J., Pryce, B., Johnson, R., Tabin, C., Schweitzer, R. and Zelzer, E. (2009). Bone ridge patterning during musculoskeletal assembly is mediated through SCX regulation of Bmp4 at the tendon-skeleton junction. *Developmental cell* **17**, 861-873.

Chen, J. W. and Galloway, J. L. (2014). The development of zebrafish tendon and ligament progenitors. *Development (Cambridge, England)* **141**, 2035-2045.

DeLaurier, A., Schweitzer, R. and Logan, M. (2006). Pitx1 determines the morphology of muscle, tendon, and bones of the hindlimb. *Dev Biol* **299**, 22-34.

Diogo, R., Abdala, V., Aziz, M. A., Lonergan, N. and Wood, B. A. (2009). From fish to modern humans--comparative anatomy, homologies and evolution of the pectoral and forelimb musculature. *J Anat* **214**, 694-716.

Edom-Vovard, F. and Duprez, D. (2004). Signals regulating tendon formation during chick embryonic development. *Developmental dynamics : an official publication of the American Association of Anatomists* **229**, 449-457.

Gilbert, S. F. (2010). *Developmental biology* (9th edn). Sunderland, Mass.: Sinauer Associates.

Gubbels, S. P., Woessner, D. W., Mitchell, J. C., Ricci, A. J. and Brigande, J. V. (2008). Functional auditory hair cells produced in the mammalian cochlea by in utero gene transfer. *Nature* **455**, 537-541.

Hama, H., Kurokawa, H., Kawano, H., Ando, R., Shimogori, T., Noda, H., Fukami, K., Sakaue-Sawano, A. and Miyawaki, A. (2011). Scale: a chemical approach for fluorescence imaging and reconstruction of transparent mouse brain. *Nature neuroscience* **14**, 1481-1488.

Huang, A., Riordan, T., Wang, L., Eyal, S., Zelzer, E., Brigande, J. and Schweitzer, R. (2013). Repositioning forelimb superficialis muscles: tendon attachment and muscle activity enable active relocation of functional myofibers. *Developmental cell* **26**, 544-551.

Huang, A. H. (2017). Coordinated development of the limb musculoskeletal system: Tendon and muscle patterning and integration with the skeleton. *Dev Biol*.

Huang, A. H., Riordan, T. J., Pryce, B., Weibel, J. L., Watson, S. S., Long, F., Lefebvre, V., Harfe, B. D., Stadler, H. S., Akiyama, H., et al. (2015). Musculoskeletal integration at the wrist underlies the modular development of limb tendons. *Development* **142**, 2431-2441.

Kardon, G. (1998). Muscle and tendon morphogenesis in the avian hind limb. *Development* **125**, 4019-4032.

Lejard, V., Brideau, G., Blais, F., Salingcarnboriboon, R., Wagner, G., Roehrl, M. H., Noda, M., Duprez, D., Houillier, P. and Rossert, J. (2007). Scleraxis and NFATc regulate the expression of the pro-alpha1(I) collagen gene in tendon fibroblasts. *J Biol Chem* **282**, 17665-17675.

Logan, M., Martin, J. F., Nagy, A., Lobe, C., Olson, E. N. and Tabin, C. J. (2002). Expression of Cre Recombinase in the developing mouse limb bud driven by a Prxl enhancer. *Genesis* **33**, 77-80.

Madisen, L., Zwingman, T. A., Sunkin, S. M., Oh, S. W., Zariwala, H. A., Gu, H., Ng, L. L., Palmiter, R. D., Hawrylycz, M. J., Jones, A. R., et al. (2010). A robust and high-throughput Cre reporting and characterization system for the whole mouse brain. *Nat Neurosci* **13**, 133-140.

Murchison, N., Price, B., Conner, D., Keene, D., Olson, E., Tabin, C. and Schweitzer, R. (2007). Regulation of tendon differentiation by scleraxis distinguishes force-transmitting tendons from muscle-anchoring tendons. *Development (Cambridge, England)* **134**, 2697-2708.

Pryce, B., Brent, A., Murchison, N., Tabin, C. and Schweitzer, R. (2007). Generation of transgenic tendon reporters, ScxGFP and ScxAP, using regulatory elements of the scleraxis gene. *Developmental dynamics : an official publication of the American Association of Anatomists* **236**, 1677-1682.

Schweitzer, R., Chyung, J. H., Murtaugh, L. C., Brent, A. E., Rosen, V., Olson, E. N., Lassar, A. and Tabin, C. J. (2001). Analysis of the tendon cell fate using Scleraxis, a specific marker for tendons and ligaments. *Development* **128**, 3855-3866.

Shinohara, H. (1999). The musculature of the mouse tail is characterized by metameric arrangements of bicipital muscles. *Okajimas folia anatomica Japonica* **76**, 157-169.

Shwartz, Y., Viukov, S., Krief, S. and Zelzer, E. (2016). Joint Development Involves a Continuous Influx of Gdf5-Positive Cells. *Cell Rep* **15**, 2577-2587.

Soeda, T., Deng, J., de Crombrugghe, B., Behringer, R., Nakamura, T. and Akiyama, H. (2010). Sox9-expressing precursors are the cellular origin of the cruciate ligament of the knee joint and the limb tendons. *Genesis (New York, N.Y. : 2000)* **48**, 635-644.

Sugimoto, Y., Takimoto, A., Akiyama, H., Kist, R., Scherer, G., Nakamura, T., Hiraki, Y. and Shukunami, C. (2013). Scx+/Sox9+ progenitors contribute to the establishment of the junction between cartilage and tendon/ligament. *Development (Cambridge, England)* **140**, 2280-2288.

Walthall, J. C. and Ashley-Ross, M. A. (2006). Postcranial myology of the California newt, Taricha torosa. *The anatomical record. Part A, Discoveries in molecular, cellular, and evolutionary biology* **288**, 46-57.

Wang, L., Jiang, H. and Brigande, J. V. (2012). Gene transfer to the developing mouse inner ear by in vivo electroporation. *J Vis Exp*.

Watson, S., Riordan, T., Pryce, B. and Schweitzer, R. (2009). Tendons and muscles of the mouse forelimb during embryonic development. *Developmental dynamics : an official publication of the American Association of Anatomists* **238**, 693-700.

Yoshimoto, Y., Takimoto, A., Watanabe, H., Hiraki, Y., Kondoh, G. and Shukunami, C. (2017). Scleraxis is required for maturation of tissue domains for proper integration of the musculoskeletal system. *Sci Rep* **7**, 45010.

Figures

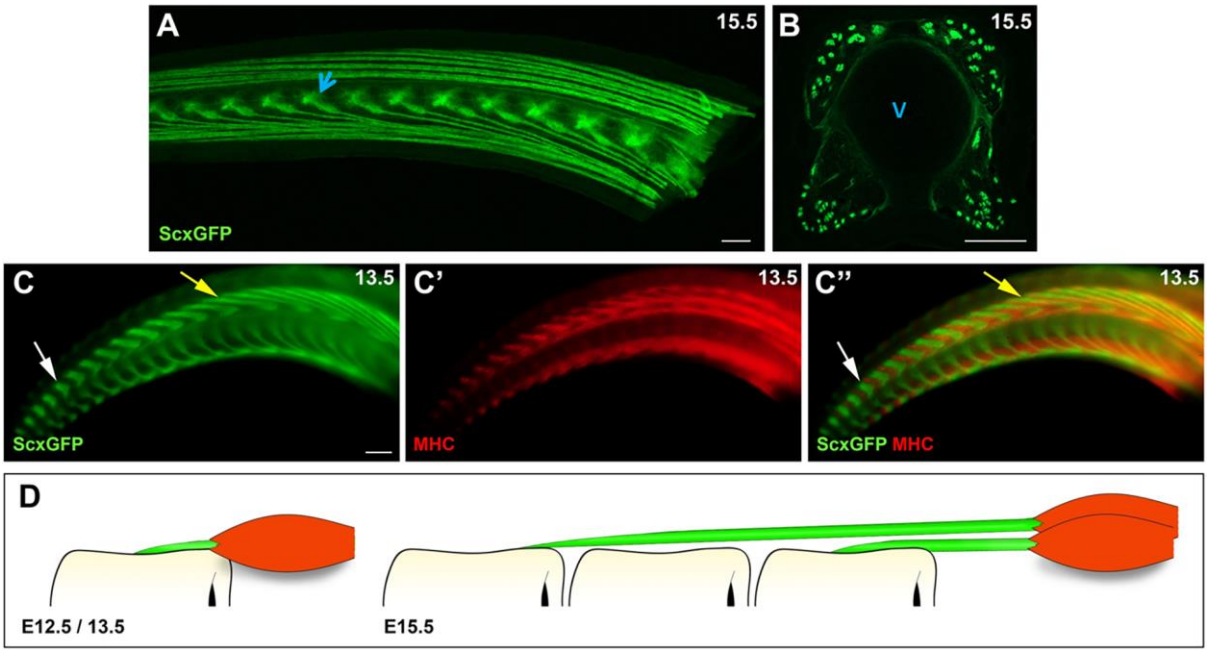

Figure 1: Long tail tendons develop via anchoring and elongation. (**A**) Whole mount confocal and (**B**) transverse section images of long tail tendons from *ScxGFP* embryos at E15.5. (**C**) Whole mount confocal images of short range tail tendon anlage from *ScxGFP* embryos at E13.5. **C'** and **C''** show whole mount staining with MHC for muscle and *ScxGFP* and MHC overlays, respectively. (**D**) Schematic of short tail tendon integrating muscle with skeleton at E12.5/E13.5 and elongated long tail tendons at E15.5. Blue arrowhead indicates an example vertebral body (V). Yellow and white arrows highlight proximal and distal tendons, respectively. Scalebars: 200µm for whole mount tails; 100µm for E15.5 transverse section.

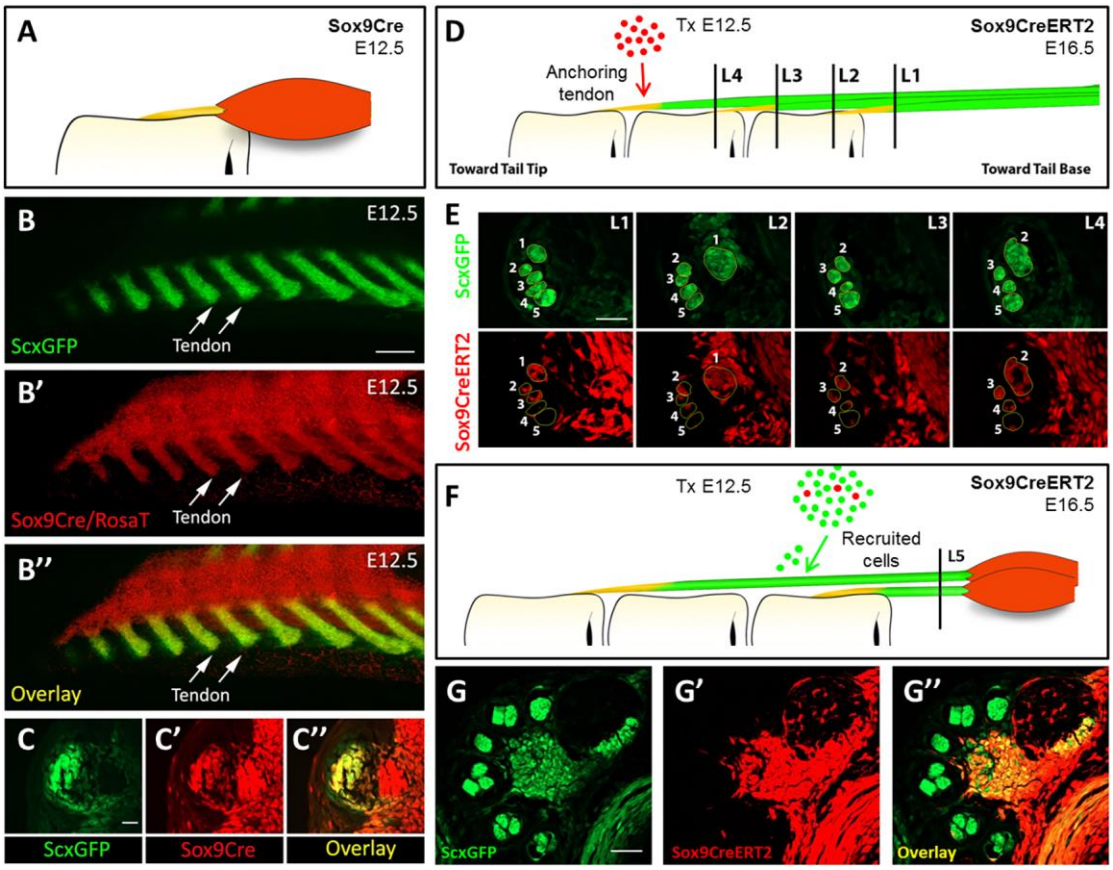

Figure 2: Tail tendon elongation is enabled by recruitment of new cells. (**A**) Schematic of *Sox9*^{lin} cell composition of short-range tail tendons labeled by *Sox9*^{Cre} at E12.5 (yellow color indicates both *ScxGFP*+ and *RosaT*+). (**B**) Whole mount confocal and (**C**) transverse section images of *Sox9*^{Cre}*; RosaT; ScxGFP* tail tendon anlage at E12.5. **B'** and **C'** show *RosaT* signal; **B"** and **C"** show *ScxGFP* and *RosaT* overlays. (**D**) Schematic of *Sox9*^{lin} composition of long tail tendons from *Sox*^{CreERT2} embryos at E16.5 (tamoxifen at E12.5) highlight *RosaT* labeling of skeletal-tendon insertions. (**E**) Transverse sections through distal tail tip of *Sox9*^{CreERT2}*; RosaT; ScxGFP* embryos at E16.5; tamoxifen was given at E12.5. Sections collected through level planes shown in **D** (L1-L4), while 1-5 labels follow specific dorsal tendons through the sections. (**F**) Schematic of *Sox9*^{lin} composition of long tail tendons from *Sox9*^{CreERT2} embryos at E16.5 (tamoxifen at E12.5) highlight absence of *RosaT* in the tendon body. (**G**) Transverse sections through tail base of *Sox9*^{CreERT2}*; RosaT; ScxGFP* embryos at E16.5; tamoxifen was

given at E12.5. Section collected through level plane L5 shown in **F**. **G'**, **G"** show *RosaT,* and *ScxGFP/RosaT* overlays, respectively. Scalebars: 200 µm for E12.5 whole mount tail; 25 µm for all transverse sections.

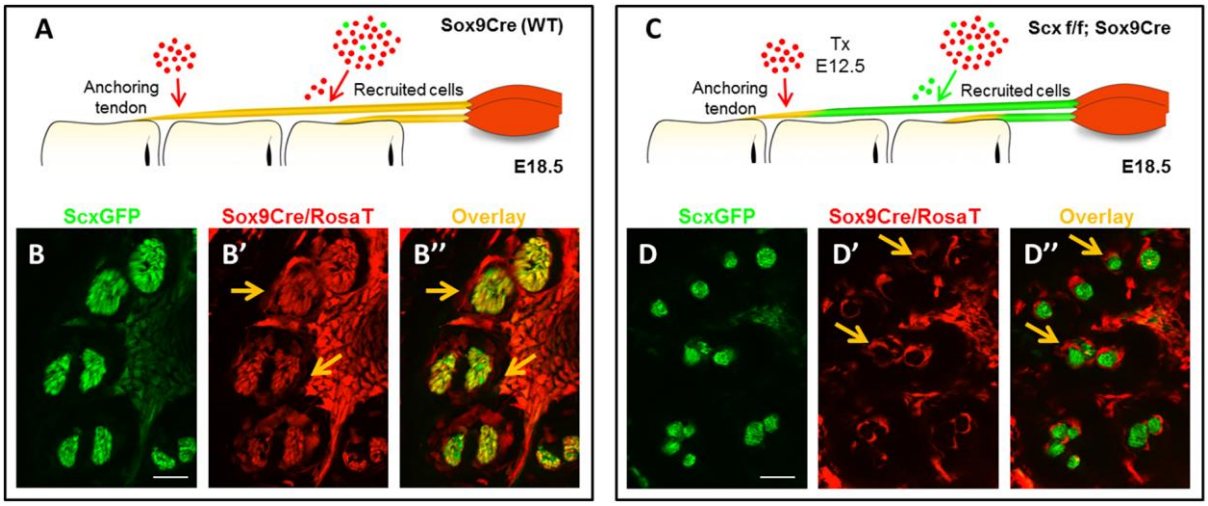

Figure 3: *Scx* is required for mesenchymal cell recruitment during tail tendon elongation. (**A**) Schematic of *Sox9*^{lin} cell composition of dorsal tail tendons labeled by *Sox9*^{Cre}*; RosaT* at E18.5. (**B**) Transverse section images of *Sox9*^{Cre}*; RosaT; ScxGFP* long dorsal tail tendons at E18.5. **B'**, **B"** show *RosaT* and *ScxGFP/RosaT* overlays, respectively. (**C**) Schematic of *Sox9*^{lin} cell composition of dorsal tail tendons of mutant *Scx*^{Sox9Cre}*; RosaT; ScxGFP* embryos at E18.5. (**D**) Transverse section images of *Scx*^{Sox9Cre}*; RosaT; ScxGFP* dorsal tail tendons at E18.5. **D'**, **D"** show *RosaT* and *ScxGFP/RosaT* overlays, respectively. Red cells indicate *Sox9*^{lin} tendon cells while green cells indicate non-*Sox9*^{lin} tendon cells. Transverse sections show tendon midsubstance regions. Orange arrows highlight *RosaT*+/*ScxGFP*- cells. Scalebars: 25 μm.

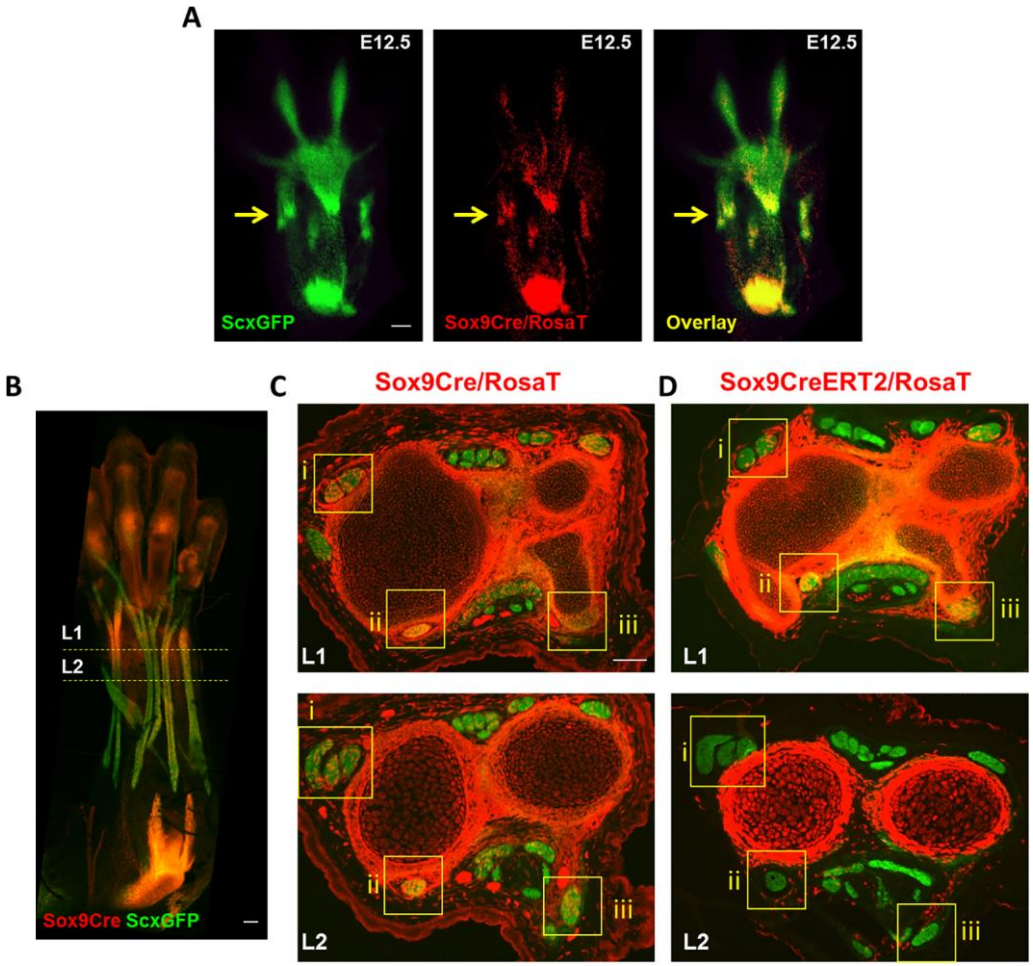

Figure 4: Limb tendon elongation is also fueled by recruitment of new progenitors. (**A**) Whole mount confocal image of *Sox9^{Cre}; RosaT; ScxGFP* forelimb at E12.5. (**B**) Whole mount confocal image of *Sox9^{Cre}; RosaT; ScxGFP* forelimb at E15.5. (**C**) Transverse section images of wild type E16.5 *Sox9^{Cre}* labeled tendons at the wrist (L1) and midsubstance (L2) levels shown in **B**. (**D**) Transverse section images of wild type *Sox9^{CreERT2}; RosaT; ScxGFP* zeugopod tendons at E16.5 (tamoxifen at E12.5) highlight *RosaT* labeling of skeletal-tendon insertions. Comparison of *Sox9^{Cre}* and *Sox9^{CreERT2}* images show that *Sox9^{lin}* cells in the tendon midsubstance are not derived from the short-range tendon but are derived from newly recruited cells. Scalebar: 200 µm (whole mount images) 100 µm (transverse sections).

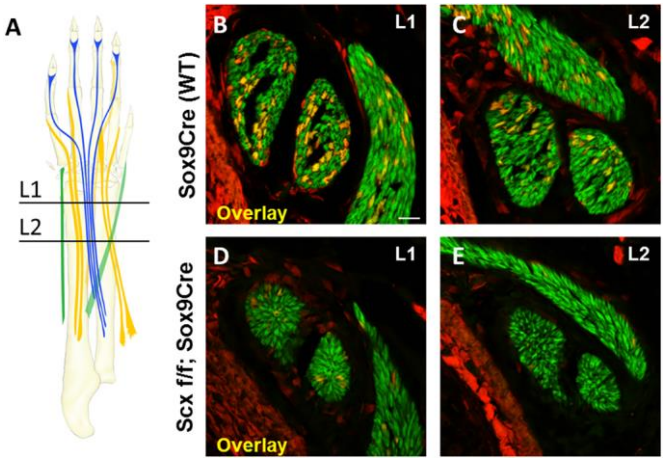

Figure 5: *Scx* is required for mesenchymal cell recruitment during limb tendon elongation. (**A**) Schematic image of extensor tendons. (**B**, **C**) Transverse section images of wild type *Sox9*^{Cre} labeled tendons at the section levels L1, L2 shown in **A**. (**D**, **E**) Transverse section images of mutant *Scx*^{Sox9Cre} tendons at the section levels L1, L2 shown in **A**. Scalebar: 20 µm.

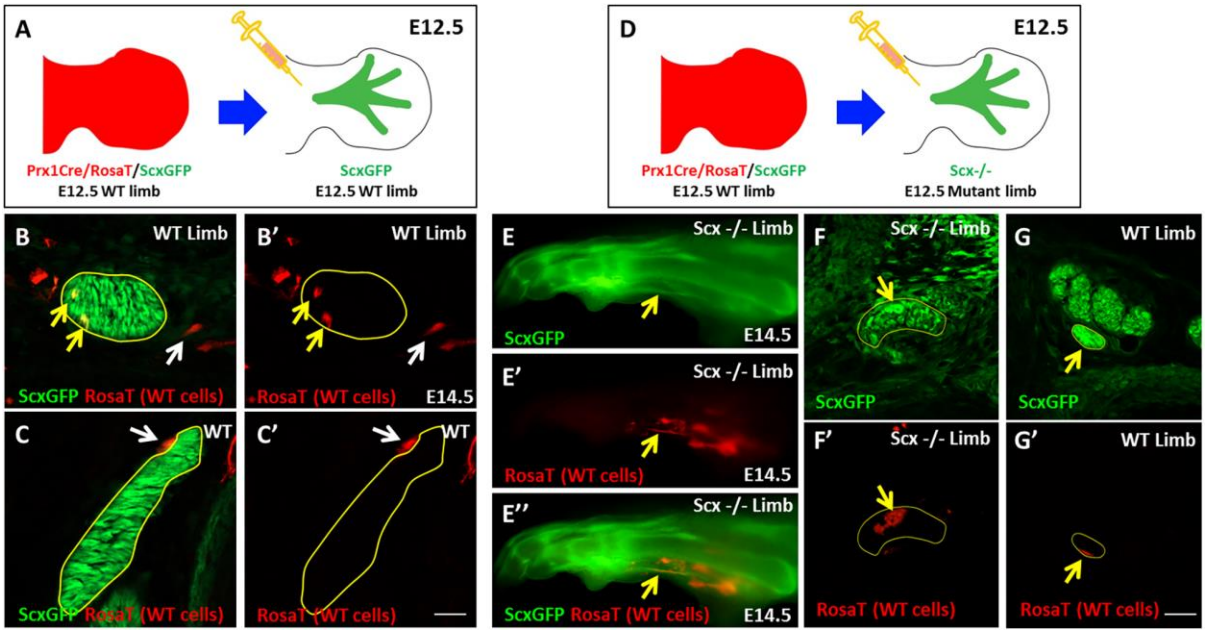

Figure 6: Transuterine microinjection of limb mesenchymal cells into stage-matched E12.5 limb buds confirms positive cell recruitment depends on *Scx* function. (**A**) Schematic of *RosaT*-labeled wild type donor cell isolation and microinjection into wild type host limbs. (**B**) Transverse section through a representative tendon showing positive recruitment of donor cells (yellow arrows, *RosaT+/ScxGFP+*) into host tendon. **B'** shows *RosaT* only. (**C**) Transverse section through a representative tendon as an example of non-recruitment, indicated by *RosaT+/ScxGFP*-negative expression (white arrow). **C'** shows *RosaT* only. (**D**) Schematic of *RosaT*-labeled wild type donor cell isolation and microinjection into mutant *Scx*$^{-/-}$ host limbs. (**E**, **E'**, **E"**) Whole mount *Scx*$^{-/-}$ limb shows extensive recruitment of WT *RosaT* donor cells into tendon (yellow arrow). (**F, F'**) Transverse sections through mutant and (**G, G'**) WT tendons show massive and minimal recruitment of WT *RosaT+/ScxGFP+* donor cells, respectively (yellow arrows). Data is representative of 26 WT embryos and 4 *Scx*$^{-/-}$ mutant embryos. Scalebars: 25 µm.

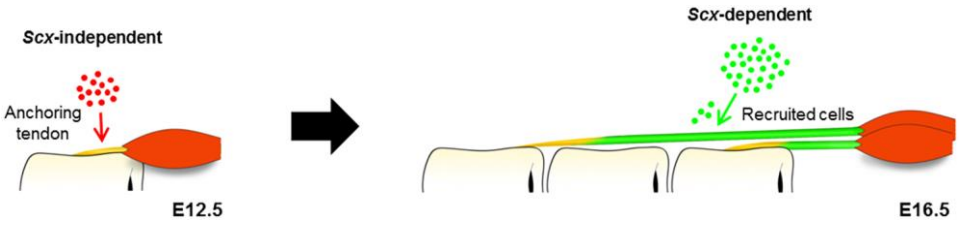

Figure 7: Model of cell recruitment and *Scx*-dependency during long tendon elongation. Schematic of *Scx*-independent anchoring and *Scx*-dependent elongation phases of long tendon development. Red cells indicate *Sox9^{lin}/ScxGFP* tendon cells that comprise the early anchoring tendon. Subsequently, tendon cells (green cells) are recruited to enable long tendon growth.

Supplemental Files

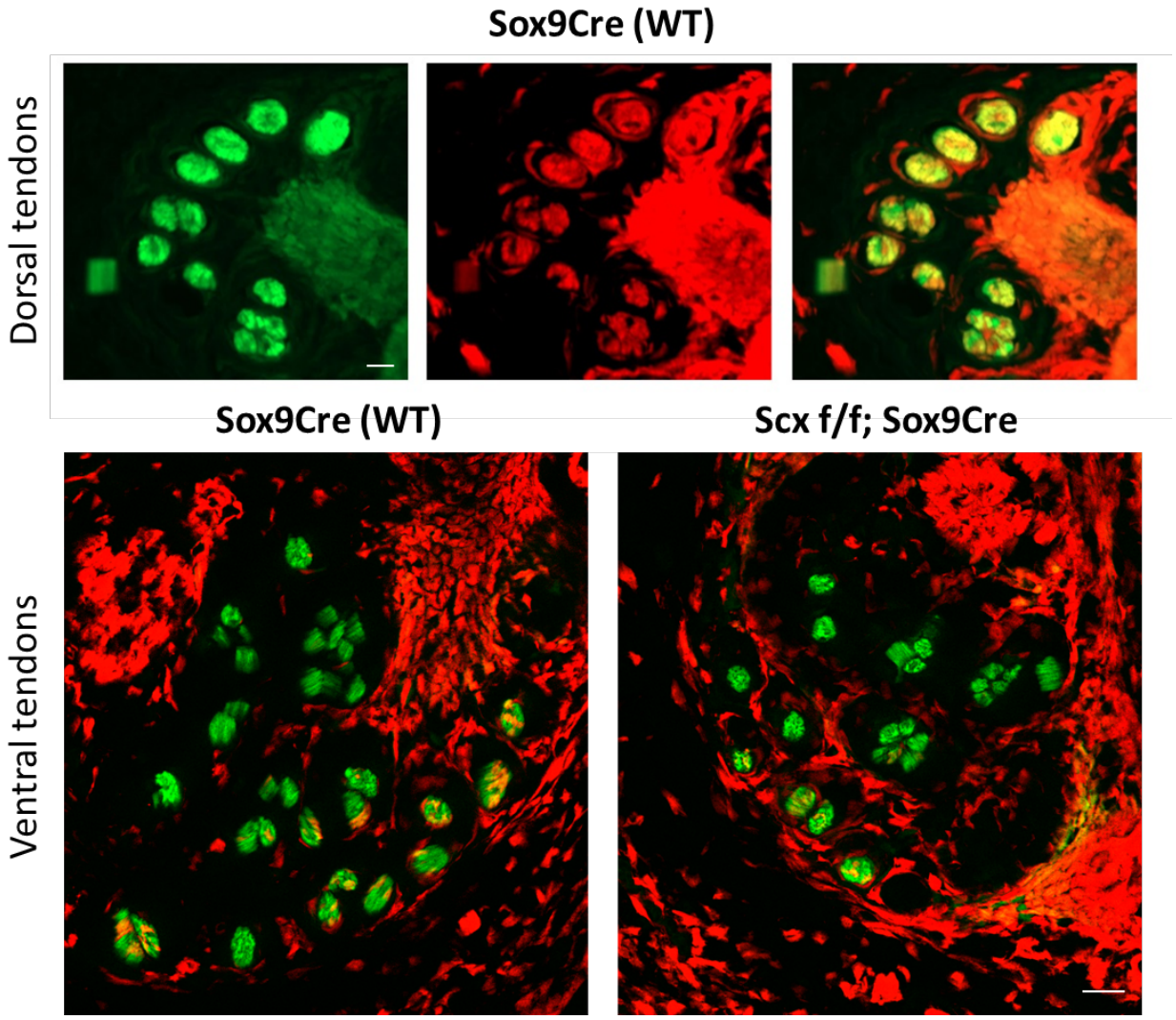

Figure S1: Lineage tracing reveals distinct contribution of *Sox9^{lin}* cells to dorsal and ventral tail tendons. Transverse sections through *Sox9^{Cre}; RosaT; ScxGFP* tails at E16.5 show that dorsal tail tendons are almost completely composed of *Sox9^{lin}* cells while ventral tail tendons are composed of a mixture of *Sox9^{lin}* and non-*Sox9^{lin}* cells. Transverse sections through *Scx^{Sox9Cre}; RosaT; ScxGFP* tails also show that mutant and wild type ventral tendons are similar in size. Scalebars: 25 μm.

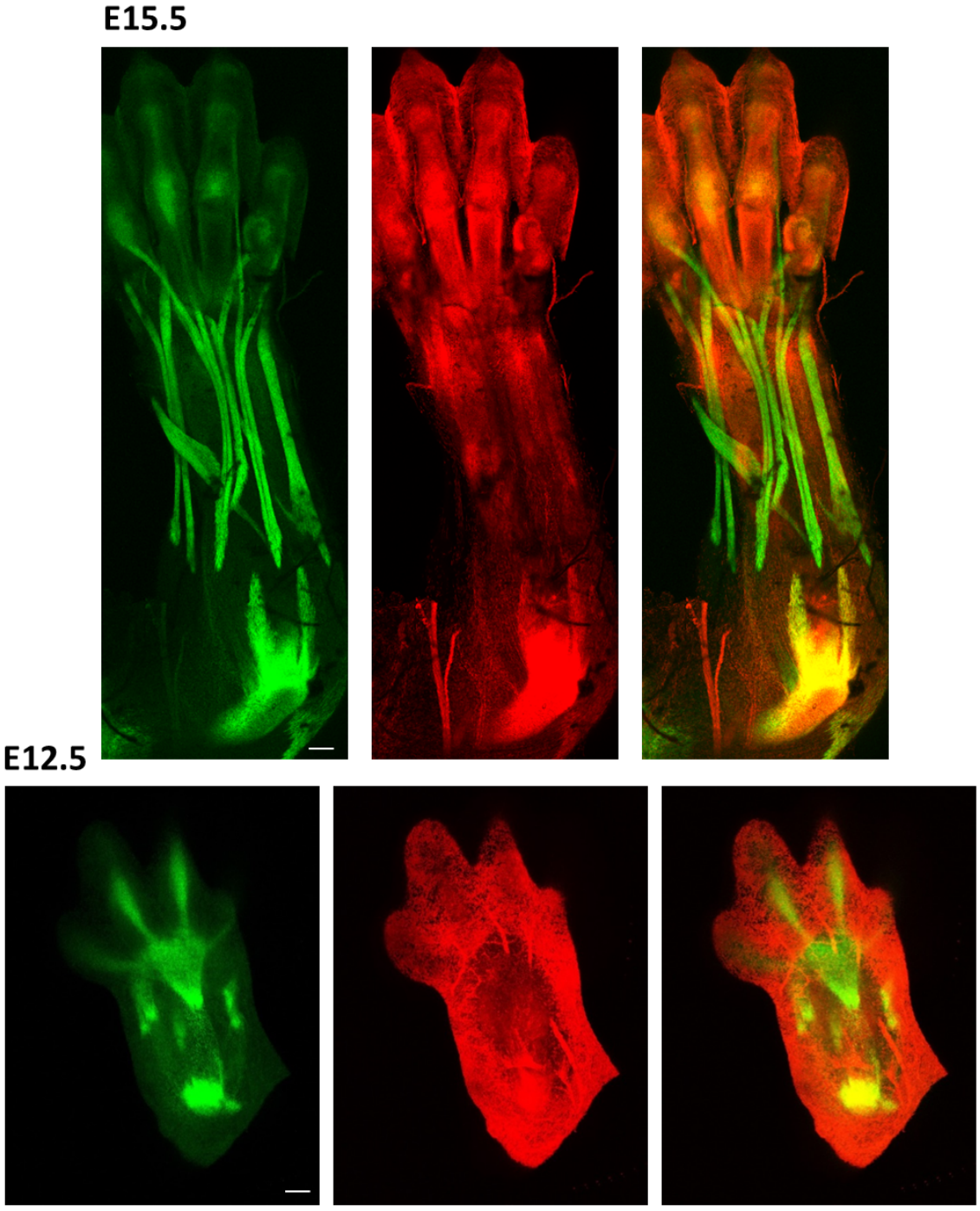

Figure S2: Unprocessed *Sox9^{Cre}; RosaT; ScxGFP* limbs at E15.5. Maximum projection images obtained from whole mount confocal microscopy shows overwhelming *RosaT* signal that is not restricted to tendon cells. Scalebars: 200 µm.

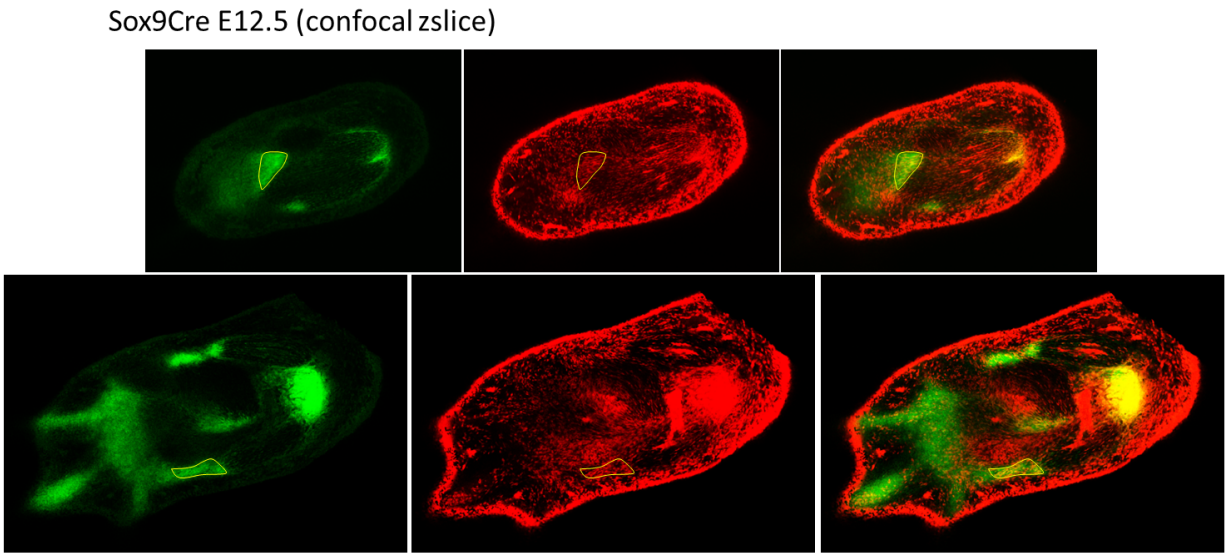

Figure S3: Unprocessed *Sox9^{Cre}; RosaT; ScxGFP* limbs at E12.5. Optical sections through the limb show concentration of *Sox9^{lin}* cells in short-range tendons near the wrist.